Properties of the linearized quantum optical bus

Robert Bruckmeier and Stephan Schiller

Fakultät für Physik, Universität Konstanz, 78457 Konstanz, Germany*

(Received 7 May 1998)

A formalism is developed that allows one to calculate the propagation of quantum noise, technical noise, and signals through a linearized *quantum optical bus*, i.e., a complex composite multibeam optical quantum system. General expressions for the output squeezing, the correlation coefficient, and quantum correlation coefficient between output observables and the transfer coefficients are derived and discussed in detail. The *total correlation* is introduced as a measure of the overall correlation of a set of output quadratures. From its geometric interpretation a multidimensional uncertainty relation is derived. *Direct* quantum-state preparation (QSP) is introduced as a method complementary to the conventional, indirect QSP. The *minimal variance* achievable by direct QSP is shown to provide superior noise suppression, including quantum noise suppression, than the conditional variance provided by indirect QSP. As an application we calculate and discuss the properties of a balanced bus of beam splitters with squeezed vacua at the usually unused ports. An important experimental effect is imperfect beam mode match, which is shown to lead to dramatic effects. A theory is derived which quantitatively matches measurements. Analytic expressions for the imperfectly modematched squeezed-light beam splitter including detection losses are given. Finally, a direct method is used to calculate the input-output matrix for the multiport subthreshold degenerate optical parametric amplifier for arbitrary parametric and mirror coupling strengths and detuning. [S1050-2947(99)02101-0]

PACS number(s): 42.50.−p

I. INTRODUCTION

In the early 1980s, tremendous theoretical progress was achieved in quantum optics, particularly on squeezed light [1,2], quantum amplifiers [3], and quantum-nondemolition (QND) measurements [4]. Soon after, paralleling experimental results on squeezing [5], QND measurements [6], twin beams [7], and quantum amplifiers [8] were accomplished. These advances sparked the definition and use of characteristic quantities to gauge the performance of the realized systems [9,10]. Recently, more complex systems have been realized that inject the output of one quantum optical system into a second quantum system [11,12].

All of this work investigated basic quantum optical properties, such as the squeezing of the output beams, the correlation coefficients between various operators, or the transfer coefficients. As experiments became more complex and their explorations were carried out in more detail, the existing theory needed to be extended in order to answer two major questions:

(i) How can quantum optical properties of composite systems be predicted, knowing the properties of the individual systems? The answer must take into account that one system may generate correlated and/or squeezed beams that are input beams of a following system.

(ii) How can the results of nonideal ''real life'' experiments be predicted? Apart from optical losses, two more effects are present in general and may affect the detection of quantum optical properties significantly: First, technical noise, e.g., from the laser source, is detected in addition to quantum noise and increases the noise level beyond quantum-mechanical limits. Second, imperfect modematch leads to the detection of several modes on a detector, and can lead to dramatic interference effects, as is demonstrated later.

This paper resolves these issues using a linearized approach, which is appropriate when weakly fluctuating, bright beams are detected. The contents of this paper are structured as follows: A formalism that allows the composition of individual quantum optical systems and the presence of technical noise is derived (Secs. II and III) and used to predict the squeezing (Sec. IV), the transfer coefficients (Sec. V), and the correlation of beam operators (Sec. VI). The total correlation is defined and introduced as a measure of the overall correlation present in a multimode system, and used to derive a multidimensional uncertainty relation (Sec. VII). A method for quantum-state preparation (QSP) is presented, which provides superior noise reduction in comparison to the conventional approach (Sec. VIII). As an application, a balanced quantum optical bus consisting of beam splitters with squeezed vacua at the usually unused ports is analyzed (Sec. IX). The theoretical model is further generalized to include imperfect modematch using a multimode description of a single beam (Sec. X). Finally a derivation of a general input-output (IO) matrix for a degenerate optical parametric amplifier is presented (Sec. XI). The paper closes with a summary and conclusions (Sec. XII). For some parts of this paper, a more detailed discussion can be found in Ref. [13].

Recently, a series of publications on QND measurements has appeared which focuses on experimental techniques, measurement results, and their comparisons to theoretical predictions [12,14,15]. In these references the correspondence between experiment and theory was remarkable. A thorough explanation of the theory used was not possible due to space limitations. In this paper the successfully applied theoretical model is explained in detail.
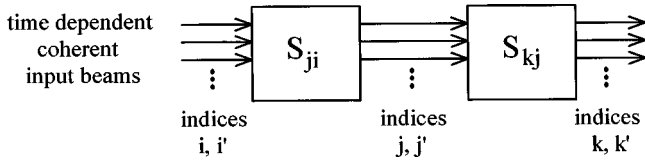
*URL: http://quantum-optics.physik.uni-konstanz.de

FIG. 1. Block diagram of the general quantum optical bus.

II. INPUT-OUTPUT FORMALISM
FOR THE QUANTUM OPTICAL BUS

To keep the notation of various quantities as simple as possible, we adopt the following convention: The name of the index of a quantity, e.g., the amplitude of a certain beam, characterizes where the quantity is located within the optical bus in accord to Fig. 1. Input quantities are indexed with i and i', the first optical system S_{ji} transforms these quantities to those indexed by j and j', which are again transformed by the next optical system S_{kj} to quantities indexed by k and k'. Whenever properties are discussed that are independent of the position within the optical bus, indices g and g' denote input beams of S_{hg}, and h and h' denote the output beams.

We consider the initial conditions that all *input* beams of the first system (indexed by i) are in time-dependent coherent states $|\alpha_i(t)\rangle$, where $\alpha_i(t)$ is a time-dependent complex function that describes an intentional modulation or technical noise. This is the special case $P_i(\beta,t)=\delta^2(\beta-\alpha_i(t))$ of the Glauber-Sudarshan distribution which directly relates to the most general time-dependent density operator $\int|\beta\rangle\langle\beta|P_i(\beta,t)d^2\beta$ for an input state. This is a good assumption for many experiments because the vacuum state is given by $\alpha_i(t)=0$ and the output of a laser driven well above threshold is a coherent state. This description allows us to include quantum and technical noise as well as an intentional signal. The connection to the lowering operators a_i is then

$$a_i(t)|\alpha_i(t)\rangle=\alpha_i(t)|\alpha_i(t)\rangle. \qquad (1)$$

Working in the corotating frame, the carrier of a beam is given by the time average of the quantum mechanical expectation value $A_g\equiv\overline{\langle a_g(t)\rangle}$. Then the fluctuations of the lowering operator and the fluctuations of the coherent excitation can be defined as $\delta a_g(t)\equiv a_g(t)-A_g$ and $\delta\alpha_g(t)\equiv\alpha_g(t)-A_g$, respectively. The Hermitian quadrature operators are defined by $X_g(t)\equiv(a_g(t)+a_g^\dagger(t))/2$ and $Y_g(t)\equiv(a_g(t)-a_g^\dagger(t))/2i$, and likewise for the fluctuation quadrature operators $\delta X_g(t)$ and $\delta Y_g(t)$, leading to

$$X_g(t)=\delta X_g(t)+\mathrm{Re}(A_g), \qquad (2a)$$

$$Y_g(t)=\delta Y_g(t)+\mathrm{Im}(A_g), \qquad (2b)$$

$$a_g(t)=A_g+\delta X_g(t)+i\,\delta Y_g(t). \qquad (2c)$$

The optical system S_{hg} transforms these input beams to output beams. In this paper we investigate systems that allow a linearized treatment of the fluctuations, which leads to IO relations [2] of the forms

$$\delta X_h(\omega)=c_{hg}(\omega)\delta X_g(\omega)+c'_{hg}(\omega)\delta Y_g(\omega), \qquad (3a)$$

$$\delta Y_h(\omega)=d'_{hg}(\omega)\delta X_g(\omega)+d_{hg}(\omega)\delta Y_g(\omega). \qquad (3b)$$

The fluctuation angular frequency is denoted by ω and the (Einstein) sum convention of free indices that occur in pairs is used. Comparing these equations to their Hermitian conjugates, it can be seen that $c_{hg}^*(\omega)=c_{hg}(-\omega)$ and the analogous relations for c', d, and d' hold, and that all four matrices are real for $\omega=0$. By selecting appropriate input and output quadratures, it is in many cases possible to simplify these expressions significantly and obtain decoupled equations for the quadratures, i.e., $c'_{hg}=0=d'_{hg}$. Then the amplitude and phase quadratures propagate independently of each other.

In general, A_h are steady-state solutions depending on the system S_{hg} and its inputs. However, if S_{hg} operates fully linear, relations (3) also hold for the full quadratures, not only for their fluctuations, and the following relation allows to determine the carrier of an output:

$$A_h=(c_{hg}(0)+id'_{hg}(0))\mathrm{Re}(A_g)+(c'_{hg}(0)+id_{hg}(0))\mathrm{Im}(A_g). \qquad (4)$$

The fundamental commutation relations $[a_g(t),a_{g'}^\dagger(t')]=\delta_{gg'}\delta(t-t')$ and $[a_g(t),a_{g'}(t')]=[a_g^\dagger(t),a_{g'}^\dagger(t')]=0$ of the raising and lowering operators express the boson character of the light field. Using $f(\omega)\equiv\int_{-\infty}^{\infty}f(t)e^{-i\omega t}dt/2\pi$ for the fourier transformation, the commutator relations

$$[a_g(\omega),a_{g'}^\dagger(\omega')]=\delta_{gg'}\delta(\omega+\omega')/2\pi,$$

$$[a_g(\omega),a_{g'}(\omega')]=[a_g^\dagger(\omega),a_{g'}^\dagger(\omega')]=0, \qquad (5a)$$

$$[X_g(\omega),Y_{g'}(\omega')]=i\delta_{gg'}\delta(\omega+\omega')/4\pi,$$

$$[X_g(\omega),X_{g'}(\omega')]=[Y_g(\omega),Y_{g'}(\omega')]=0 \qquad (5b)$$

follow, which also hold analogously for the fluctuation operators. To ensure that an optical system transforms input boson fields to output boson fields, the four IO matrices must obey further restrictions. Using Eqs. (3) and (5b) and $\omega'=-\omega$, the following matrix consistency relations are derived:

$$c(\omega)d^\dagger(\omega)-c'(\omega)d'^\dagger(\omega)=1,$$

$$c(\omega)c'^\dagger(\omega)=c'(\omega)c^\dagger(\omega), \qquad (6)$$

$$d(\omega)d'^\dagger(\omega)=d'(\omega)d^\dagger(\omega).$$

A consequence of these equations is the conservation of phase-space volume, as discussed later in this paper. For decoupled quadratures the important relation

$$c^{-1}(\omega)=d^\dagger(\omega) \qquad (7)$$

results, allowing one to deduce the properties of one quadrature type from the other. In addition this demonstrates the inverse properties of actions on the quadratures of a *single* beam: amplification of the phase comes together with deamplification of the amplitude, which eventually leads to squeezed light. For phase-insensitive amplification at least two beams must be coupled.

III. PHOTODETECTION AND PHOTOCURRENT CORRELATIONS

The statistical properties of beams are usually investigated experimentally by photodetection. The photocurrents are calculated by

$$i_h(t) = a_h^\dagger(t) a_h(t)$$
$$\approx |A_h|^2 + 2 \, \text{Re}(A_h) \delta X_h(t) + 2 \, \text{Im}(A_h) \delta Y_h(t), \quad (8)$$

where the electronic charge is set to unity, and terms quadratic in the fluctuations have been dropped, leading to a linear relation between the fluctuations of the current and the quadratures of the detected beam. These dropped terms are negligible if the fluctuations are small with respect to the carrier, i.e., for a weakly modulated, bright beam. This approximation is not applicable for single photon detection or for pulsed systems. Fourier transforming the currents and using Eq. (3) results in

$$i_h(\omega) = I_h \delta(\omega) + 2 \, \text{Re}(A_h) \delta X_h(\omega) + 2 \, \text{Im}(A_h) \delta Y_h(\omega)$$
$$= I_h \delta(\omega) + x_{hg}(\omega) \delta X_g(\omega) + y_{hg}(\omega) \delta Y_g(\omega), \quad (9)$$

with the mean current

$$I_h \equiv |A_h|^2, \quad (10)$$

$$x_{hg}(\omega) \equiv 2 \, \text{Re}(A_h) c_{hg}(\omega) + 2 \, \text{Im}(A_h) d'_{hg}(\omega), \quad (11)$$

and

$$y_{hg}(\omega) \equiv 2 \, \text{Re}(A_h) c'_{hg}(\omega) + 2 \, \text{Im}(A_h) d_{hg}(\omega). \quad (12)$$

A spectrum analyzer measures the electric power spectral density $P_h(\omega)$ of this current at a specific frequency $\omega/2\pi$. In classical physics, this power density is proportional to $|i_h(\omega)|^2$. This can be generalized to the quantum mechanical expectation value $P_h(\omega) = \langle i_h^\dagger(\omega) i_h(\omega) \rangle$ for the product state of the input beams. There is no ordering ambiguity since $i_h(\omega)$ and $i_h^\dagger(\omega')$ commute. Also, the constant of proportionality has been dropped as only ratios of power densities will be used. In the following, the more general second-order expectation value $K_{hh'}(\omega, \omega') \equiv \langle i_h^\dagger(\omega) i_{h'}(\omega') \rangle$ is calculated, which also allows one to calculate the correlation of the output currents. Some identities are very handy to evaluate these quantities: $\langle \delta X_i(\omega) \rangle = (\text{Re} \, \delta\alpha_i)(\omega)$ and $\langle \delta Y_i(\omega) \rangle = (\text{Im} \, \delta\alpha_i)(\omega)$, where the notation indicates that $(\text{Re} \, \delta\alpha_i)(\omega)$ is the Fourier transform of the real part of $\delta\alpha_i(t)$, not vice versa. Note that the index i denotes reference to the coherent input beams. To evaluate second-order expectation values such as

$$\langle \delta X_i(\omega) \delta X_{i'}(\omega') \rangle = (\text{Re} \, \alpha_i)(\omega)(\text{Re} \, \alpha_{i'})(\omega')$$
$$+ \delta_{ii'} \delta(\omega + \omega')/8\pi, \quad (13)$$

the quadratures are decomposed into creation and annihilation operators, and simplified using the commutator relation (5a), leading to the second term in Eq. (13) that will generate the quantum noise. Taking everything together, the results are

$$K_{hh'}(\omega, \omega') \equiv \langle i_h^\dagger(\omega) i_{h'}(\omega') \rangle$$
$$= \langle i_h(\omega) \rangle^* \langle i_{h'}(\omega') \rangle + (x_{hi}^*(\omega) x_{h'i}(\omega)$$
$$+ i x_{hi}^*(\omega) y_{h'i}(\omega) - i y_{hi}^*(\omega) x_{h'i}(\omega)$$
$$+ y_{hi}^*(\omega) y_{h'i}(\omega)) \delta(\omega - \omega')/8\pi, \quad (14)$$

$$P_h(\omega) \equiv \langle i_h^\dagger(\omega) i_h(\omega) \rangle$$
$$= |\langle i_h(\omega) \rangle|^2 + \sum_i |x_{hi}(\omega) + i y_{hi}(\omega)|^2 \delta(0)/8\pi, \quad (15)$$

$$\langle i_h(\omega) \rangle = I_h \delta(\omega) + x_{hi}(\omega)(\text{Re} \, \delta\alpha_i)(\omega)$$
$$+ y_{hi}(\omega)(\text{Im} \, \delta\alpha_i)(\omega). \quad (16)$$

Note that there is an explicit reference to the input beams via the index i, since their quantum properties are known by Eq. (1). The terms in Eq. (15) may be interpreted as follows: The first term is the power spectral density of the classical photocurrent (16), where $I_h \delta(\omega)$ generates the power of the dc photocurrent and the second and third terms in Eq. (16) generate the ac photo current due to a classical modulation of the input beam caused by the Fourier components of $\delta\alpha_i$. The second term in Eq. (15) is the quantum noise that originates from the commutation relations and that is present even when $\delta\alpha_i = 0$. The appearance of the δ functions reflects the integration of the electrical current over all times in the Fourier transform.

These expressions are very general, and include all the quantum mechanics that is necessary to proceed further. Many systems, however, show their optimum properties when the quadratures are decoupled, i.e., $c' = d' = 0$. In the rest of this paper, we will focus on these systems. When two of these systems, S_{kj} and S_{ji}, are combined, $c_{ki} = c_{kj} c_{ji}$, $d_{ki} = d_{kj} d_{ji}$ and $c'_{ki} = d'_{ki} = 0$ result for the composite system S_{ki}. To ensure that the photodetectors only register one quadrature, we consider X_h and Y_h to be the amplitude and phase quadratures, respectively. This is expressed in $\text{Im}(A_h) = 0$ as seen from Eq. (8). $\text{Im}(A_h) = 0$, and

$$A_h = c_{hg}(0) A_g \quad (17)$$

follows from $\text{Im}(A_g) = 0$ and Eqs. (4) if the system S_{hg} is fully linear. Then $\text{Im}(A_h) = 0$ can be achieved by injecting the input beams with appropriate phase, $\text{Im}(A_g) = 0$. In practice, this is done using servo control systems. In addition, we assume $\omega, \omega' \neq 0$, from which $\delta X_h(\omega) = X_h(\omega)$ and $\delta Y_h(\omega) = Y_h(\omega)$ follow. Significant simplifications arise and lead to

$$i_h(\omega) = x_{hg}(\omega) X_g(\omega),$$
$$x_{hg}(\omega) = 2 A_h c_{hg}(\omega), \quad y_{hg}(\omega) = 0, \quad (18)$$

$$K_{hh'}(\omega, \omega') = 4 A_h A_{h'} \langle X_h(\omega) X_{h'}(\omega') \rangle$$
$$= A_h A_{h'} (m_h^*(\omega) m_{h'}(\omega') \delta(0)$$
$$+ c_{hi}^*(\omega) c_{h'i}(\omega) \delta(\omega - \omega'))/2\pi, \quad (19)$$

$$P_h(\omega) = I_h\left(|m_h(\omega)|^2 + \sum_i |c_{hi}(\omega)|^2\right)\delta(0)/2\pi, \quad (20)$$

where

$$m_i(\omega) \equiv \sqrt{8\pi/\delta(0)}(\mathrm{Re}\,\delta\alpha_i)(\omega), \quad m_h(\omega) \equiv c_{hi}(\omega)m_i(\omega). \tag{21}$$

The important quantity m_i denotes classical amplitude fluctuations of $\alpha_i(t)$ due to intentional modulation or technical noise. It is normalized such that $m_i = 1$ represents equal spectral power densities of the classical and the quantum noise for a time-dependent coherent state. The appearance of $\delta(0)$ in the denominator is unusual, but can be motivated as follows: If Fourier transformation is not taken for all times but only from $-T$ to $+T$, we have $\delta(0) = 2T$ and $(\mathrm{Re}\,\delta\alpha_i)(\omega)$ is proportional to $\sqrt{T}$ for white noise, which ensures that $m_i(\omega)$ is well-behaved as $T \to \infty$. As expected, only amplitude quadratures X_h, classical amplitude modulations $\mathrm{Re}\,\delta\alpha_i$ and the IO matrix c_{hi} enter the previous relations, whereas their counterparts Y_h, $\mathrm{Im}\,\delta\alpha_i$ and d_{hi} do not contribute.

Based on the previous equations, we now turn to quantities such as squeezing, transfer coefficients, and correlation coefficients which are of crucial interest in theory and experiment. From here on, equations will be presented in the frequency domain, and the argument ω is often omitted.

IV. SQUEEZING

To calculate the squeezing of an output beam h, the actual noise power density P_h of the detector current is compared to the noise power density $P_{h,\mathrm{SQL}}$ of an unmodulated, coherent beam of the same intensity and wavelength which defines the standard quantum limit, (SQL). As the current fluctuations are proportional to the amplitude fluctuations, this approach is equivalent to calculating the squeezing by comparing the variances of the amplitude fluctuations instead of the currents. To calculate $P_{h,\mathrm{SQL}}$, $\delta\alpha_i = 0$ is used for unmodulated input beams, and the "identity" optical system is considered, $c_{hi} = d_{hi} = \delta_{hi}$, $c' = d' = 0$, which leads to $P_{h,\mathrm{SQL}} = I_h\delta(0)/2\pi$. Therefore the degree of squeezing is

$$S_h \equiv \frac{P_h}{P_{h,\mathrm{SQL}}} = \frac{\langle \delta X_h^\dagger \delta X_h\rangle}{\langle \delta X_h^\dagger \delta X_h\rangle_{\mathrm{SQL}}}$$

$$= |m_h|^2 + \sum_i |c_{hi}|^2$$

$$\equiv \left|\sum_i c_{hi}m_i\right|^2 + \sum_i |c_{hi}|^2, \tag{22}$$

where the definitions of m_h and the sum convention is made explicit. The two noise terms in this expression represent technical or modulation noise and the quantum noise, respectively, transferred from the input beams to the output beam h. An important difference between modulation or technical noise and quantum noise is that modulation noise can interfere destructively, whereas quantum noise is always present. This difference is expressed by a coherent sum of the modulation amplitude contributions from different input beams and incoherent sums for the quantum noise power contribu-

tions. $S_h < 1$ indicates the generation of squeezed light and requires low classical noise and use of a system with $\Sigma_i|c_{hi}|^2 < 1$. Note that in experiments squeezing usually denotes noise *suppression*, S_h^{-1}.

At this point we wish to point out a peculiarity: Quantum concepts are used here for the definition of the initial state and for the photodetection process which involves the commutation relations. The propagation of the operators, as expressed in the IO relations, is classical: The operators themselves propagate just as their classical analogs, i.e., their quantum-mechanical average values. However, an IO matrix that satisfies the condition $|c_{hi}|^2 < 1$ is a necessary condition for a system that generates squeezed light. This demonstrates that even the classical part of a system, i.e., its input-output relations, can be responsible for nonclassical properties of the whole system, such as the detection of squeezed light.

V. TRANSFER COEFFICIENTS

A. Definition

The transfer coefficients are of central interest for the quality of information transmission. They are defined as the fraction of the input signal-to-noise power ratio (SNR) that is transferred to the output of the optical system [9]. For this purpose, a separation of the total modulation $m_g = m_g^t + m_g^s$ into broadband technical noise m_g^t and the intentional sinusoidal signal modulation m_g^s is required. The photocurrent power, when averaged over a certain bandwidth, is proportional to $|m_h^s|^2 + |m_h^t|^2 + \Sigma_i|c_{hi}|^2$, because the cross term between m_g^t and m_g^s can be shown to be negligible. Therefore the signal to noise ratio of a signal on beam h, $\mathcal{R}_h$, is

$$\mathcal{R}_h = \frac{|m_h^s|^2}{|m_h^t|^2 + \sum_i |c_{hi}|^2} = \frac{|m_h^s|^2}{S_h}, \tag{23}$$

where S_h must obviously be measured with the signal modulation turned off. For the measurement of the transfer coefficient T_{kj} from beam j to beam k a signal is only applied to the input beam j, therefore $|m_k^s|^2 = |c_{kj}|^2|m_j^s|^2$ holds. The general transfer coefficient is then

$$T_{kj} \equiv \frac{\mathcal{R}_k}{\mathcal{R}_j} = \frac{|c_{kj}|^2 S_j}{S_k}. \tag{24}$$

This relation leads to the important interpretation that the transfer coefficient is the fraction of the output noise of beam k that is due to input j. This relation can be used to determine the modulus of any coefficient of the IO matrix c_{kj}, since the squeezings can be measured independently.

B. Total transfer coefficient and phase sensitivity

For information transmission purposes it is essential to know how well the SNR can be transmitted from the emitter to the individual receivers. A suitable quantity is the total transfer coefficient

$$T_{\mathrm{tot},j} \equiv \sum_k T_{kj}, \tag{25}$$

which measures how efficient information can be transferred from a specific input j to all outputs k.

This quantity is difficult to investigate in general form. Some insight can be gained by considering phase-insensitive systems. These systems, like the beam splitter or the nondegenerate optical parametric amplifier (OPA), operate similarly on amplitude and phase noise. In contrast, a degenerate OPA reduces the noise of one quadrature at the expense of increasing the other's. A criterion for phase insensitive operation of a system is that uncorrelated input beams with phase insensitive noise (i.e., equal phase and amplitude noise for each beam) lead to output beams that still exhibit phase-insensitive noise. From this, $|c_{kj}| = |d_{kj}|$ can be concluded. The maximum total transfer coefficient for any phase-insensitive system coupling *two* beams is found to be

$$\max_{\text{phase insensitive}} T_{\text{tot},j} = \frac{2S_j}{S_{j'} + S_j}, \tag{26}$$

where S_j and $S_{j'}$ are the squeezings of the two input beams. This is shown by parametrizing the IO matrices in accord with Eq. (7) and maximizing $T_{\text{tot},j}$. The maximum is achieved for a system as simple as the balanced (50% reflectivity) beam splitter. It is important to realize that the noise of the signal input plays an important role: If the second, "meter", input is in the vacuum state ($S_{j'} = 1$), strong technical noise on the signal input ($S_j \gg 1$) will lead to an almost perfect SNR transmission ($T_{kj} \to 1$, $T_{\text{tot},j} \to 2$). This, however, is not achieved due to a smart coupling system, but because the quantum noise of the meter input, which is added to the output beams, is negligible in comparison to the signal input noise.

Quantum nondemolition measurements rely on phase-sensitive methods that allow one to measure one quadrature precisely to the expense of adding noise on the other quadrature. Phase-sensitive operation can therefore be concluded if

$$T_{\text{tot},j} > \frac{2S_j}{1 + S_j}, \tag{27}$$

as either the system itself operates phase sensitively or the meter input is squeezed ($S_{j'} < 1$) and therefore phase sensitive. The widely used criterion $T_{\text{tot},j} > 1$ for a quantum optical tap (QOT) is a special case of for $S_j = 1$ and is inapplicable if $S_j > 1$. Therefore we suggest use of Eq. (27) instead of $T_{\text{tot},j} > 1$ in future experiments to judge QOT operation.

For a general system that couples n (two or more) beams, maximizing $T_{\text{tot},j}$ for a phase-insensitive system is a complex task even for $n = 3$. The limit L for a criterion for phase-sensitive operation $T_{\text{tot},j} > L$ is still unclear. The special case of a signal beam coupled to $n - 1$ vacuum beams by beam splitters (BS) of optimal reflectivity demands

$$T_{\text{tot},j} > L_{\text{BS}} \equiv n S_j / (n - 1 + S_j), \tag{28}$$

which can be derived from Eq. (64). A different phase-insensitive test system is a high-gain nondegenerate OPA (NDOPA) with a vacuum idler input followed by $n - 2$ beam splitters that couple the outputs to vacuum. This suggests

$$T_{\text{tot},j} > L_{\text{NDOPA}} \equiv n S_j / (S_j + 1), \tag{29}$$

a limit which coincides with L_{BS} for $n = 2$ and exceeds L_{BS} for $n > 2$.

The concept of phase sensitivity has proven very successful for a categorization of two-beam systems. However, one has to realize that a combination of phase-insensitive devices may still generate squeezed states: One example is a frequency-degenerate, type-II phase-matched (polarization nondegenerate) OPA that is sandwiched between two appropriately aligned wave plates that mix signal and idler beams. The complete system is equivalent to two independent degenerate OPA's which are phase sensitive and generate squeezed light. Therefore the phase-insensitive amplifier, which is commonly—and we believe incorrectly—considered a classical device, can also exhibit nonclassical features. The two systems that lead to the criteria (28) and (29) are suitable benchmark systems. For $n \geq 3$ both criteria are different, and it is up to the experimenter to decide which system to use as a reference system.

VI. CORRELATION

A. Definition

An additional important and experimentally accessible quantity is the correlation coefficient between two beams, in the following simply termed correlation. The discussion of its properties can mediate much understanding of quantum optical systems. The correlation between the two photocurrents of beams k and k' is easily calculated:
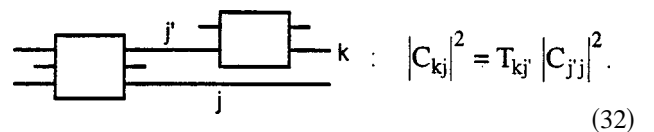
$$C_{kk'} = \frac{K_{kk'}(\omega, \omega)}{\sqrt{K_{kk}(\omega, \omega) K_{k'k'}(\omega, \omega)}} = \frac{\kappa_{kk'}}{\sqrt{S_k S_{k'}}}, \tag{30}$$

where

$$\kappa_{kk'} \equiv m_k^* m_{k'} + c_{ki}^* c_{k'i}, \tag{31}$$

which satisfies $\kappa_{kk} = S_k$. The coefficients $\kappa_{kk'}$ after the system S_{kj} are related to the coefficients $\kappa_{jj'}$ before the system by $\kappa_{kk'} = c_{kj}^* c_{k'j'} \kappa_{jj'}$. Thus, a correlation $C_{kk'} \neq 0$ for $k \neq k'$ can be due to either a common modulation or to the condition $c_{ki}^* c_{k'i} \neq 0$, which expresses a rare and precious quantum correlation ability of the system, as shown below.

For the correlation between two beams j and k, the expressions are analogous to Eq. (30), where k' is replaced by j. In this situation we have $\kappa_{kj} = c_{kj}^* \kappa_{j'j}$. An interesting special case arises, when the implicit sum of the latter expression consists of only one term, i.e. if there is only one (fixed) beam j' that is correlated to beam j and is connected to beam k. In this situation, which is sketched below, one obtains

$$\left| C_{kj} \right|^2 = T_{kj'} \left| C_{j'j} \right|^2. \tag{32}$$

This equation states that a correlation is propagated through a system with the same efficiency as a classical signal, namely, the transfer coefficient.

If all beams j are uncorrelated, $\kappa_{jj'} = \delta_{jj'} S_j$, all information is then present in the absolute noise level, i.e., the

squeezing, and no reference to the initial beams i is required. It is therefore not surprising that significant simplifications arise:

$$S_k = \sum_j |c_{kj}|^2 S_j, \tag{33}$$

$$T_{kj} = |c_{kj}|^2 S_j / S_k \quad \text{(as before)}, \tag{34}$$

$$\kappa_{kk'} = \sum_j c_{kj}^* c_{k'j} S_j \quad \text{and} \quad C_{kk'} = \kappa_{kk'} / \sqrt{S_k S_{k'}}, \tag{35}$$

$$\kappa_{kj} = c_{kj}^* S_j \quad \text{and} \quad |C_{kj}|^2 = T_{kj}. \tag{36}$$

This leads to the conclusion that measurements of the squeezing, the transfer coefficients, and the correlation do not allow one to distinguish between classical and quantum noise.

From Eqs. (33) and (34), it can be concluded that the sum of the transfer coefficients *to one output* is unity, $T_{k,\text{tot}} \equiv \Sigma_j T_{kj} = 1$. This is not surprising as T_{kj} can be interpreted as the fraction of noise power originating from beam j that contributes to the total noise power present in beam k. However, this does not limit the total transfer coefficient $T_{\text{tot},j} \equiv \Sigma_k T_{kj}$, the sum of transfer coefficients *from one input*.

Equation (36) allows a different interpretation of the transfer coefficients, namely, that they are the modulus square of the correlation coefficient between input and output fluctuations. The assumption of uncorrelated input beams to that system is essential. A counterexample is two correlated input beams that are passed unchanged through a system. Obviously every output is correlated with every input, but two transfer coefficients that are unity, the other two vanish.

A crucial question is: How can correlation be generated? There are three different routes to prepare correlated beams k and k': (i) Two input beams $j \neq j'$ are already correlated: $\kappa_{jj'} \neq 0$. (ii) Two input beams j and j' carry different noises: $S_j \neq S_{j'}$. (iii) The system S_{kj} possesses the *entanglement property*: $\exists\, k \neq k'$: $c_{kj}^* c_{k'j} \neq 0$. If none of these conditions is satisfied, their negations $\kappa_{jj'} = S_j \delta_{jj'}$, $S_j = S_{j'}$ and $c_{kj}^* c_{k'j} = |c_{kj}|^2 \delta_{kk'}$ quickly lead to $\kappa_{kk'} = S_k \delta_{kk'}$, which states that no output correlation is present. Obviously, the first method is not constructive, as it makes use of already correlated beams. The second is best illustrated with a simple example: Consider a modulated beam (squeezing is greater than 1) incident on a beam splitter, the other input is the vacuum state (the squeezing is equal to 1). Both output beams are then correlated due to their common modulation. However, it is shown in the next paragraph that this correlation is of classical origin. Quantum correlation can only be generated by (iii).

B. Quantum correlation and entanglement

One of the most interesting features of quantum mechanics is the concept of entanglement. This section differentiates between correlation and quantum correlation [16]. The first may be caused completely by a classical correlation, i.e., a correlation of the expectation values, whereas the second is related to entanglement. One indicator for entanglement is the correlation of the quantum fluctuations of two operators in different Hilbert spaces: If there is no entanglement between these spaces, then the total state, or more generally the total density operator, allows factoring off these two spaces, and then the correlation vanishes. Therefore, an observation of correlated quantum fluctuations requires the presence of entanglement.

Let us investigate the quantum correlations of the photocurrents. Pure quantum correlations are calculated using $\langle a,b \rangle \equiv \langle \Delta a \Delta b \rangle = \langle ab \rangle - \langle a \rangle \langle b \rangle$, where quantities of the type $\Delta a \equiv a - \langle a \rangle$ are investigated to remove classical fluctuations. The superscript Q is used to denote that exclusively quantum properties are considered. The quantum correlation is then

$$C_{kk'}^Q \equiv \frac{K_{kk'}^Q}{\sqrt{K_{kk}^Q K_{k'k'}^Q}}, \tag{37}$$

where

$$K_{kk'}^Q(\omega,\omega') \equiv \langle i_k^+(\omega), i_{k'}(\omega') \rangle$$
$$= K_{kk'}(\omega,\omega') - \langle i_k(\omega) \rangle^* \langle i_{k'}(\omega') \rangle. \tag{38}$$

Using Eq. (14), it is easily seen that the quantum correlation is the same as the correlation when no modulation or technical noise is present ($\delta \alpha_i = 0$). The remaining terms originate from commutation relations which again states their true quantum nature. Together with Eq. (19), the following is easy to see for the decoupled case discussed in the latter part of the paper:

$$K_{kk'}^Q(\omega,\omega') = A_k A_{k'} c_{ki}^* c_{k'i} \delta(\omega - \omega')/2\pi. \tag{39}$$

Therefore, entangled states can be generated by a device that exhibits the *entanglement property*

$$\exists\ k \neq k': c_{ki}^* c_{k'i} \neq 0. \tag{40}$$

The properties of quantum correlation were derived in the frequency domain, but the time domain is also of interest. Using Fourier transformation and Eq. (39) one can derive $\langle i_k(t), i_{k'}(t') \rangle = A_k A_{k'} \int c_{ki}^*(\omega) c_{k'i}(\omega) e^{-i\omega(t-t')} d\omega/2\pi$. This leads to the quantum correlation coefficient in the time domain:

$$C_{kk'}^Q(t,t') = \frac{\int c_{ki}^* c_{k'i} e^{-i\omega(t-t')} d\omega}{\sqrt{\int c_{ki}^* c_{ki} d\omega}\sqrt{\int c_{k'i}^* c_{k'i} d\omega}}. \tag{41}$$

As is to be expected, temporal correlation can be observed over time differences which are inverse to the bandwidth over which $c_{ki}^* c_{k'i}$ is significant.

C. Testing for quantum correlation

For an experimenter one important question is whether a measured correlation is due to entanglement or to technical

noise in the system. This section derives bounds for the quantum correlation coefficient, which are experimentally accessible. All input beams to the system are assumed to be uncorrelated, and all beams j except for beam j_0 exhibit a squeezing of unity, such as vacuum. This situation applies if only one laser beam that carries technical noise is injected into a system. Using the inequalities $|a-b|^2 \gtrless (|a| \mp |b|)^2$, the following holds:

$$\left| \sum_j c_{kj}^* c_{k'j} \right|^2 = \left| \left(\sum_j c_{kj}^* c_{k'j} S_j \right) - c_{kj_0}^* c_{k'j_0} (S_{j_0} - 1) \right|^2 \gtrless S_k S_{k'} (|C_{kk'}| \mp \sqrt{T_{kj_0} T_{k'j_0}} \varepsilon)^2, \tag{42}$$

$$S_k^Q \equiv \sum_j |c_{kj}|^2 = S_k (1 - T_{kj_0} \varepsilon), \tag{43}$$

where $\varepsilon \equiv 1 - 1/S_{j_0}$. For the quantum correlation it immediately follows that

$$|C_{kk'}^Q|^2 = \frac{\left| \sum_j c_{kj}^* c_{k'j} \right|^2}{\sum_j |c_{kj}|^2 \sum_j |c_{k'j}|^2} \gtrless \frac{(|C_{kk'}| \mp \sqrt{T_{kj_0} T_{k'j_0}} \varepsilon)^2}{(1 - T_{kj_0} \varepsilon)(1 - T_{k'j_0} \varepsilon)}. \tag{44}$$

Therefore, the presence of a quantum correlation and hence entanglement may be concluded from measurements of the input squeezing, the correlation coefficient, and the transfer coefficients. For small excess input noise, i.e., small ε, the correlation and the quantum correlation are nearly identical: $C_{kk'}^Q = C_{kk'} + O(\varepsilon)$. As the lower bound for $|C_{kk'}^Q|^2$ never becomes negative, care has to be taken when both terms in the numerator of the lower bound are comparable within measurement error.

VII. TOTAL CORRELATION

A. Definition

In this section we introduce a quantity that describes the full extent of the correlation present in a system. The conditional variance $V_{k|M}$ discussed below is not appropriate, as it treats the prepared and measured output beams differently, and neglects the phase quadratures. There is a different approach that takes all quadratures into account on the same basis. All quadratures are denoted by Q_h, where the index h specifies the beam and the quadrature type, e.g., amplitude or phase. To describe the full correlation present in a system we introduce a new quantity, the total correlation C_{tot}:

$$C_{\text{tot}}^2 \equiv 1 - \text{Det } C_{hh'}, \tag{45}$$

where $C_{hh'} \equiv \kappa_{hh'} / \sqrt{\kappa_{hh} \kappa_{h'h'}}$ is the matrix of correlation coefficients between the quadratures Q_h and $Q_{h'}$. As the general quadratures do not commute, a symmetrized product is used for the second moment:

$$\kappa_{hh'} \equiv \frac{4\pi}{\delta(0)} \langle Q_h^\dagger Q_{h'} + Q_{h'} Q_h^\dagger \rangle. \tag{46}$$

The antisymmetric part of $Q_h^\dagger Q_{h'}$ is omitted here: Since it is the commutator of the operators and is independent of the state under investigation it cannot reveal information about it. The resulting Hermitian matrix κ is normalized such that a diagonal element κ_{hh} equals the squeezing S_h of the operator $Q_h : \kappa_{hh} = S_h$.

The total correlation exhibits the following desired properties: (1) All quadratures and beams are treated equally. (2) $0 \leq C_{\text{tot}}^2 \leq 1$. (3) C_{tot}^2 is invariant under complex scaling of each quadrature operator. (4) $C_{\text{tot}}^2 = 1$ if any two quadratures are perfectly correlated. (5) C_{tot}^2 remains invariant if new uncorrelated quadratures are included. (6) $C_{\text{tot}}^2 = |C_{12}|^2$ for the case of two quadratures, where C_{12} is their correlation coefficient. Except for the second relation, which is proven below, these relations are simple consequences of the definitions. The diagonals of the Hermitian matrix $C_{hh'}$ are unity, and its trace equals its dimension. According to definition (46), diagonalizing $C_{hh'}$ is interpreted as finding eigenquadratures from linear combinations of Q_h that are uncorrelated in pairs. A consequence is that the eigenvalues of $C_{hh'}$ are positive because they are the variances of the respective eigenquadratures. Therefore the determinant of $C_{hh'}$ is positive and $C_{\text{tot}}^2 \leq 1$ holds. Furthermore, the sum of all (positive) eigenvalues equals the trace of $C_{hh'}$. As a consequence, the determinant is at most unity, from which $C_{\text{tot}}^2 \geq 0$ follows. This measure does not distinguish between having two or more perfectly correlated quadratures, as in both cases $C_{\text{tot}} = 1$. To distinguish these cases, the dimension minus the rank of the correlation matrix is a good measure, as it denotes the number of perfectly squeezed quadratures that can ideally be obtained.

The geometric interpretation of the determinant as a multidimensional volume offers additional insight. First we motivate the concept using a two-dimensional example, where Q_1 and Q_2 are the correlated amplitude and phase quadratures of a state. The joint measurement probability of the *normalized* quadratures is represented in Fig. 2 as a density of points.

The plotted ellipse is a suitable contour line of the measurement density. $C_{hh'}$ is completely specified by the correlation coefficient between the quadratures, i.e., $\frac{15}{17}$ in the example shown in Fig. 2. The uncorrelated eigenquadratures are oriented at 45° and 135° and their variances of $\frac{32}{17}$ and $\frac{2}{17}$ are given by the eigenvalues of $C_{hh'}$ according to above reasoning. The half axes of the ellipse are the square roots of these eigenvalues. The area of the rotated rectangle that
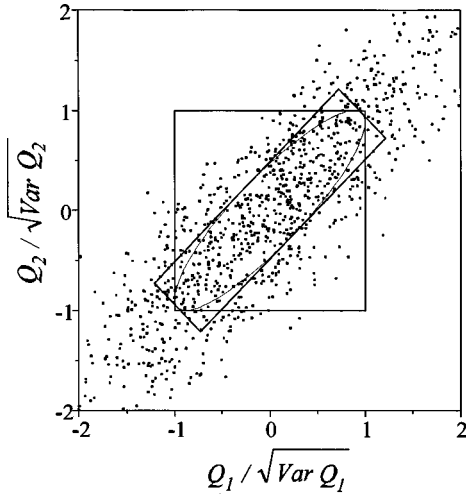
FIG. 2. Representation of the uncertainty volume. For descriptions, see text.

bounds the ellipse can be expressed compactly by $4\sqrt{\text{Det } C_{hh'}}$, which is at most 4 for uncorrelated quadratures. Therefore, $\sqrt{\text{Det } C_{hh'}} = \sqrt{1 - C_{\text{tot}}^2}$ is the fraction of the maximum uncertainty volume which is accessed by the normalized quadratures. The total correlation therefore is a measure for the confinement of the uncertainty volume accessed by the normalized quadratures due to correlations present.

B. Multidimensional uncertainty relation

The concept of an uncertainty volume is linked to Heisenberg's uncertainty relation. Using the ideas of Sec. VII A a generalized uncertainty relation is derived. A linear optical system transforms the input quadratures Q_j to output quadratures Q_k according to

$$Q_k = M_{kj} Q_j,$$

where

$$|\text{Det } M| = 1. \tag{47}$$

This relation reexpresses Eqs. (3a) and (3b), where the condition on the IO matrix M is seen from the matrix consistency relations cast in matrix form:

$$\begin{pmatrix} c & c' \\ -d' & -d \end{pmatrix} \begin{pmatrix} d & -d' \\ c' & -c \end{pmatrix}^{\dagger} = 1, \quad M = \begin{pmatrix} c & c' \\ d' & d \end{pmatrix}. \tag{48}$$

Equation (47) asserts that the uncertainty volume is kept constant during the transformation.

Note that classical noise is still included in this description. The operation of a modulator that can generate optical fluctuations is interpreted as follows: The optical system is coupled to an additional mode, usually of electric nature, which is the input for the fluctuations that are transferred to the optical beam in a process conserving the uncertainty volume. In the subspace that excludes this additional mode, the uncertainty volume may increase.

For the derivation of the generalized uncertainty relation uncorrelated input quadratures are considered, $\kappa_{jj'} = S_j \delta_{jj'}$, from which Det $\kappa_{jj'} = \Pi_j S_j$ results. From Eqs. (47) and (46)

follows Det $\kappa_{kk'} = \text{Det}(M_{kj}^{+} \kappa_{jj'} M_{k'j'}) = \Pi_j S_j$, and from Eqs. (45) and (46) $1 - C_{\text{tot}}^2 = \text{Det } C_{kk'} = \text{Det } \kappa_{kk'} / \Pi_k S_k$. First we conclude that

$$(1 - C_{\text{tot}}^2) \prod_k S_k = \prod_j S_j \tag{49}$$

which asserts that the left-hand side is invariant during the propagation, which restates the conservation of uncertainty volume. Next we deduce the multidimensional uncertainty relation

$$\prod_k S_k = \frac{\prod_j S_j}{1 - C_{\text{tot}}^2} \geq \frac{1}{1 - C_{\text{tot}}^2} \geq 1. \tag{50}$$

The first inequality results from the usual two-dimensional uncertainty relation $S_g^X S_g^Y \geq 1$ between the amplitude noise S_g^X and the phase noise S_g^Y for each individual beam, which can be derived from Eq. (5b). The second arises because the total correlation is between zero and 1. The left side of Eq. (50) is the product of the variances of all quadratures, which cannot fall below unity. If these quadratures are correlated, this product is at least $(1 - C_{\text{tot}}^2)^{-1} > 1$. This important statement expresses that the uncertainty *product* (not volume) of correlated quadrature observables is *strictly larger* than the uncertainty product of its eigenquadratures or the minimum uncertainty product. This situation is depicted in Fig. 2: The uncertainty volume accessed by Q_1 and Q_2 is bounded closer by the rotated rectangle, relating to the eigenquadratures, than by the square.

Finally, we consider the special case of decoupled amplitude and phase quadratures. Then both the correlation matrix and the IO matrix decouple, and the total correlation can be factored to two total correlations for the amplitude and phase correlations. The decoupled uncertainty relation now reads

$$\prod_k S_k^X S_k^Y = \frac{\prod_j S_j^X}{1 - C_{\text{tot}}^{X2}} \frac{\prod_j S_j^Y}{1 - C_{\text{tot}}^{Y2}} \geq 1. \tag{51}$$

The indices now denote just the beam, whereas the quadrature type is specified explicitly by the superscripts X and Y for amplitude and phase, respectively.

VIII. QUANTUM-STATE PREPARATION (QSP)

The aim of a quantum state preparator is to provide a quantum state where the variance of a specific observable is as small as possible. The border line to successful QSP is crossed if that variance is below the standard quantum limit. This can be achieved by either directly generating a squeezed state ("direct" QSP) or by generating a state and delivering additional information that can be used to predict the observable for that specific state to better than the SQL ("indirect" QSP). The choice of the attributes "direct" and "indirect" reflects the fact that for indirect QSP additional information is required and obtained by a measurement process in contrast to direct QSP. Sections VIII A and VII B investigate both indirect and direct QSP's and their relation.

A. Indirect QSP: measurement and correction

Consider an optical system that generates entangled output beams. Each measurement of an output beam leads to a state reduction of the full state, by which the states of the other output beams are changed. This is interpreted as state preparation of these beams. The quality of the state preparation for output beam k is characterized by the conditional variance $V_{k|M}$, which is the remaining variance of the observable X_k, having measured all observables $X_{k'}$ of beams $k' \in M$ specified by set M of (measured) beams and using the information from these measurements to predict X_k. Interestingly, QSP does not rely on entanglement, as any noise may be reduced in one quantity given other *correlated* quantities—classical or quantum correlation being equally useful.

In the following, a linear system is considered, and Gaussian fluctuations are assumed, which allow important simplifications. In particular, the conditional variance does not depend on the specific values $X_{k'}$ measured. Also, the conditional variance can then be calculated by minimizing the variance of the sum of the observable X_k and a linear combination of the other measured observables, where the coefficients $g_{k'}$ are optimized:

$$V_{k|M} = \min_{g_{k'}} \frac{\text{Var}\left(X_k - \sum_{k' \in M} g_{k'} X_{k'} \right)}{\delta(0)/8\pi}. \tag{52}$$

The normalization is identical to that of the squeezing [Eq. (13)], which requires $V_{k|M} = S_k$ when no measurements are performed on other beams, i.e., for $M = \{\ \}$. The best conditional variance can obviously be achieved by measuring all other output beams. If the intermediate quadratures X_j are uncorrelated, further results can be easily derived. The optimum linear combination is given by $g_{k'} = \kappa_{k'k''}^{-1} V_{k''}$, where $V_{k'} \equiv \kappa_{k'k}$ and $\kappa_{k'k''}^{-1}$ is understood as the inverse of the matrix that is indexed only by members of M. Then the conditional variance is

$$V_{k|M} = S_k - V_{k'}^* \kappa_{k'k''}^{-1} V_{k''} = S_k(1 - C_{\text{QSP},k|M}^2), \tag{53}$$

$$C_{\text{QSP},k|M}^2 \equiv V_k^* \kappa_{k'k''}^{-1} V_{k''}/S_k. \tag{54}$$

This result was previously derived in Ref. [10], and a closely related discussion can also be found in Ref. [17]. For the special case of two output beams, where beam 1 is prepared and beam 2 is measured, this simplifies to the well known result $V_{1|\{2\}} = S_1(1 - |C_{12}|^2)$. For the case of three beams, indirect QSP results in

$$C_{\text{QSP},1|\{2,3\}}^2 = \frac{|C_{12}|^2 + |C_{13}|^2 - 2\,\text{Re}\,C_{12}C_{23}C_{31}}{1 - |C_{23}|^2}. \tag{55}$$

The total correlation (45) is $C_{\text{tot}}^2 = |C_{12}|^2 + |C_{23}|^2 + |C_{31}|^2 - 2\,\text{Re}\,C_{12}C_{23}C_{31}$ for three quadratures. Together with Eq. (55) one finds that the total correlation exceeds the QSP correlation: $C_{\text{tot}}^2 \geq C_{\text{QSP},1|\{2,3\}}^2$.

Interpreting Eq. (53), one finds that good state preparation, i.e., low $V_{k|M}$, is achieved when the beam to be pre-
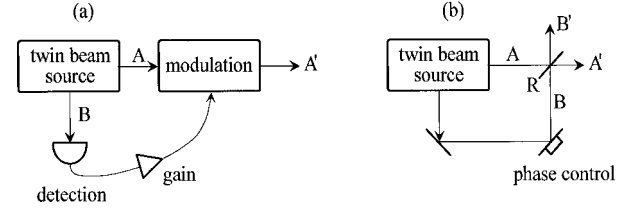

FIG. 3. Comparison of two types of QSP. (a) Conventional indirect QSP by detection and appropriate modulation. (b) Direct QSP by mixing of beams A and B with an appropriate beam splitter.

pared already exhibits low noise S_k before QSP. Furthermore, this noise level can be reduced by the factor $1 - C_{\text{QSP},k|M}^2$ due to the correlation coefficient $C_{\text{QSP},k|M}$ between the prepared observable X_k and the optimal prediction $\Sigma_{k' \in M} g_{k'} X_{k'}$ derived from the measured observables $X_{k'}$. X_k can be transformed to $X_k - \Sigma_{k' \in M} g_{k'} X_{k'}$ using a modulator, appropriately driven by the measurement results $X_{k'}$. The squeezing of this output beam is then given by the conditional variance $V_{k|M}$. This method was applied successfully to the twin-beam output of a nondegenerate optical parametric oscillator (OPO) by Mertz *et al.* [18] to generate squeezed light and to demonstrate its QSP ability [Fig. 3(a)]. Most schemes avoid the optical feed-forward modulator and use electronic noise reduction after the measurement of X_k to take advantage of quantum noise reduction [7,19].

Indirect QSP effectively uses the transformation $X_k \rightarrow X_{\text{shear},k} \equiv X_k - \Sigma_{k' \in M} g_{k'} X_{k'}$ to prepare a quadrature of low variance. If Q_1 and Q_2 of Fig. 2 are considered amplitude quadratures, the transformation $Q_1 \rightarrow Q_1 - g_2 Q_2$ pictorially corresponds to *shearing* the density distribution horizontally. For optimal g_2 the transformed ellipse in Fig. 2 is vertically aligned, i.e., the new variance of Q_1 is minimal (using shear transformations) and equals the conditional variance before the transformation. The variance of Q_2 remains unchanged as Q_2 is not transformed.

B. Direct QSP: rotation in quadrature space

However, there is a better method for QSP: *rotating* instead of shearing. For optimal rotation angle, the ellipse of Fig. 2 ends up in the vertical position as for shearing transformation. However, for the price of an increased variance of Q_2, this will reduce the variance of Q_1 below the conditional variance, and permit improved QSP beyond the reach of conventional indirect QSP. Note that the rotation takes place in true quadrature space, not in the normalized quadrature space depicted in Fig. 2. The beauty of this method is that the required rotation can be realized by a simple beam splitter, as indicated in Fig. 3(b).

More generally, we define the *minimal variance* V_R as the lowest squeezing of a single amplitude quadrature that can be achieved by rotation of the amplitude quadratures specified by a set R:

$$V_R \equiv \min_{\text{rotation } \tilde{g}_{k'}} \frac{\text{Var}\left(\sum_{k' \in R} \tilde{g}_{k'} X_{k'} \right)}{\delta(0)/8\pi}. \tag{56}$$

This relates directly to expression (52) of the *conditional*

variance $V_{k|M}$ when $R=\{k\}\cup M$ is used. The minimization in V_R is constrained to rotations, which satisfy $\Sigma_{k'\in R}|\tilde{g}_{k'}|^2 =1$. The required rotation $X_k\rightarrow X_{\mathrm{rot},k}\equiv\Sigma_{k'\in R}\tilde{g}_{k'}X_{k'}$ can be realized experimentally by mixing beam k with all beams indexed by $M=R\backslash\{k\}$ using phase control and beam splitters of appropriate reflectivity.

The relative contributions of the individual quadratures to the considered output are equal for both indirect and direct QSP's. However, the absolute scale is different due to the different constraints in V_R and $V_{k|M}$. This leads directly to

$$V_R=\frac{V_{k|M}}{1+\displaystyle\sum_{k'\in M}|g_{k'}|^2}\leq V_{k|M}, \qquad (57)$$

where $g_{k'}$ denote the optimized coefficients that apply for $V_{k|M}$ [Eq. (52)]. A geometric interpretation of the quadrature rotation reveals that the rotation angles are chosen to transform the joint probability density such that minimal variance emerges for the selected output quadrature. Therefore the output quadrature is the eigenquadrature of the second-moment matrix κ with lowest eigenvalue, i.e., minimal noise. This leads to the conclusion that the minimal variance is given by the minimal eigenvalue of κ:

$$V_R=(\mathrm{min\ eigenvalue\ }\kappa_{k'k''}),$$

where

$$k',k''\in R. \qquad (58)$$

We can compare direct and indirect QSP for the two-beam case indicated in Fig. 3. Let S_A and S_B be the squeezings of the beams A and B', their correlation is denoted C. Their conditional variances are then $V_{A|\{B\}}=S_A(1-|C|^2)$ and $V_{B|\{A\}}=S_B(1-|C|^2)$. The minimal variance $V_{\{A,B\}}$ and the required optimized reflectivity R of the beam splitter are

$$V_{[A,B]}=\frac{S_A+S_B}{2}-\left[\left(\frac{S_A-S_B}{2}\right)^2+S_AS_B|C|^2\right]^{1/2}, \quad (59)$$

$$R=\frac{1}{2}+\frac{S_A-S_B}{4\left[\left(\dfrac{S_A-S_B}{2}\right)^2+S_AS_B|C|^2\right]^{1/2}}. \qquad (60)$$

We give one example to show the potential of QSP by rotation. A high-gain nondegenerate OPA is known to generate twin beams with high correlation $C\rightarrow 1$ and identical noise level $S\equiv S_A=S_B$. In this case one expects $V_{\{A,B\}}=S(1-|C|)$ which is lower than both conditional variances by the factor $1+|C|$. In frequency-degenerate systems [20] direct QSP can therefore outperform indirect QSP by up to 3 dB of quantum noise reduction. This method may come along with a destructive interference of the carriers of the input beams. However, when frequency-dependent elements like a cavity are inserted in one input beam, both destructive interference of the noise and constructive interference of the carriers is possible and minimal noise and maximal output power are achieved.

The advantages of direct versus indirect QSP are (i) a superior noise suppression, (ii) operation at an optical rather
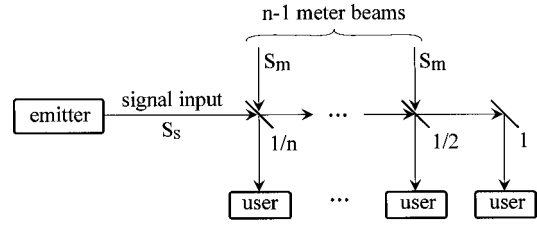

FIG. 4. Balanced information transmission system. The signal input is distributed to n users using $n-1$ beam splitters of indicated reflectivities. The squeezings of the signal and meter inputs are S_s and S_m, respectively.

than an electronic bandwidth, (iii) a very low insertion loss, and (iv) the possibility to recycle the laser power of the second output from the beam splitter. The detection inefficiency for indirect QSP plays a similar role as imperfect modematch for direct QSP.

Finally, implications for the categorization of systems emerge: A system that exhibits $V_{k|M}<1$, which is conventionally termed the QSP criterion, can be used to generate squeezed light. That system is therefore considered a nonclassical device. However, a system that is incapable of *indirect* QSP, $V_{k|M}\geq 1$, may still provide squeezed light using *direct* QSP if $V_R<1$. Therefore, instead of the *conditional variance* $V_{k|M}$ the *minimal variance* V_R should be used to classify a system as classical ($V_R\geq 1$) or nonclassical ($V_R<1$).

IX. APPLICATION: BALANCED QUANTUM OPTICAL BUS CONSISTING OF BEAM SPLITTERS WITH SQUEEZED VACUA AT THE USUALLY UNUSED PORTS

One purpose for a quantum optical bus is to transport the optical information of a signal beam from one emitter to a specific number of receivers n. The simplest way to achieve this is to use a sequence of beam splitters to generate the number of required outputs for the receivers. We consider an arbitrary topology of the beam splitters, e.g., linear or binary-tree-like, but require that every one of the output beams receives an equal share of the input information. To make use of quantum noise reduction, we consider equally squeezed vacuum incident at the usually unused input ports of the beam splitters. The fluctuations of all input beams are therefore independent. An example for such a system is given in Fig. 4, which was discussed in Ref. [21].

To calculate the properties of this system, it is divided into two parts. The first system S_{ji} treats every beam separately. The signal, whose squeezing is S_s, is passed unchanged, and every other input which is in the vacuum state is squeezed, such that the resulting squeezing is S_m. One important parameter is the fraction of meter to signal noise $\sigma\equiv S_m/S_s$. The next system S_{kj} describes the mixing of these beams by the beam splitters. This is a unitary transformation, and therefore $c_{kj}^*c_{k'j}=\delta_{kk'}$ and $c_{kj}^*c_{kj'}=\delta_{jj'}$ hold. The requirement of equal signal distribution is implemented by $|c_{kj}|^2=1/n$ if $j=1$, which denotes the signal beam. Using the expressions of the previous paragraphs, the following results are obtained for this system:

$$S_k = S_s(\sigma + (1-\sigma)/n), \qquad (61)$$

$$|C_{kk'}| = \left| \frac{1-\sigma}{n\sigma + (1-\sigma)} \right| \quad \text{for } k \neq k', \qquad (62)$$

$$T_{k1} = \frac{S_s}{nS_k} = \frac{1}{n\sigma + (1-\sigma)}, \qquad (63)$$

$$T_{\text{tot},1} = \frac{S_s}{S_k} = \frac{1}{\sigma + (1-\sigma)/n}. \qquad (64)$$

The total transfer coefficient $T_{\text{tot},1}$, which is the crucial parameter for information transmission, goes to $1/\sigma$ as n becomes large. This leads to the surprising result that as far as information transmission is considered, instead of using $n-1$ squeezers, it is just as efficient to use a single anti-squeezer, such as a noiseless parametric amplifier, to generate a signal input beam with a squeezing of $1/\sigma$, and to use vacuum at all meter input ports. As $\sigma < 1$, this amplified beam carries excess noise, which increases the noise floor at the input and helps to achieve a good $T_{\text{tot},1}$. Interestingly, there is no difference whether this excess noise is due to increased quantum noise or to classical noise. However, using a noiseless parametric amplifier to antisqueeze the signal before it is injected into the beamsplitter array does not affect the SNR at the input, and increases the SNR at each output.

Further calculations provide the results for the remaining quantities of interest. Preparing one beam and measuring all others, the conditional variance is

$$V_{k|\text{rest}} = \frac{n\sigma}{n+\sigma-1}, \qquad (65)$$

which goes along with a QSP correlation of

$$C^2_{\text{QSP},k|\text{rest}} = \frac{(n-1)(1-\sigma)^2}{(n+\sigma-1)(\sigma n - \sigma + 1)}. \qquad (66)$$

Finally, the expression for the total correlation is

$$C^2_{\text{tot}} = 1 - \frac{1}{\sigma} \left[1 - \frac{1-\sigma}{(n-1)\sigma + 1} \right]^n. \qquad (67)$$

For an intuitive grasp of the dependences the previous functions are plotted in Fig. 5. Interestingly, $C_{\text{QSP},k|\text{rest}}$ decreases as more beams are included, and eventually vanishes as $n \to \infty$. As both $V_{k|\text{rest}}$ and S_k approach S_m, by Eq. (53) one finds that their quotient, $1 - C^2_{\text{QSP},k|\text{rest}}$, has to approach unity and that there is no essential correlation left.

X. EFFECTS OF IMPERFECT MODE MATCH

A. Evidence for dramatic experimental effects

During early stages of our experiments on QND measurements, the transfer coefficients were investigated for a dual-port resonator, where an input beam was partially reflected
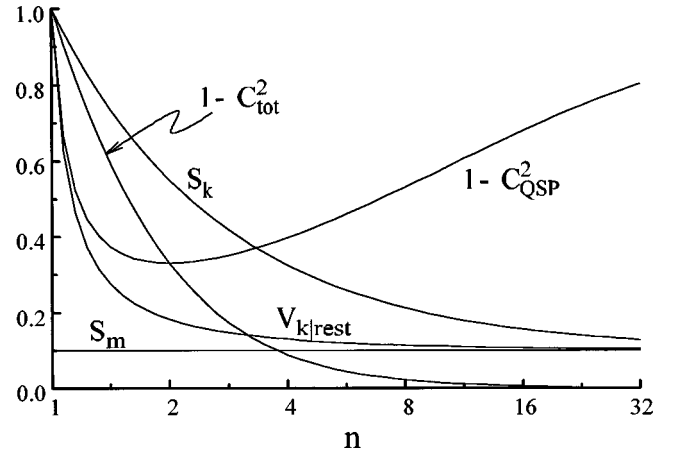
FIG. 5. Operation characteristics of the balanced quantum optical bus as indicated for $S_s = 1$ and $S_m = 0.1$.

from and partially transmitted through the cavity. To our surprise, we found dramatic discrepancies between experimental data and the predictions. This problem sparked most of the contents of this paper.

The resonator used for this experiment was a monolithic lithium niobate ring resonator with a free spectral range of 10.19 GHz, a 1.25% transmitting dielectric input coupler, and round trip losses of 0.39%. Frustrated total internal reflection was used to generate an additional coupling that could be varied by moving a coupling prism near the crystal surface with a piezoelectric transducer. The optical efficiencies were 98.5%, 96.3%, 96.6%, and 97% for the propagation of the input beam, the reflected beam, the transmitted beam, and the quantum efficiencies of the photodiodes, respectively. The single-frequency input beam was at a wavelength of 1064 nm, and its power was 2.35 mW. This system was described in detail in Ref. [14]. The measurements of the transfer coefficients in Fig. 6 were taken at a frequency of 21.5 MHz. The measured transfer coefficient for the reflected beam showed a striking and unexpected dip at an output coupling near 0.7%, as indicated by the vertical arrow.

Eventually, the imperfect mode match of 90.2% turned out as the origin of this unexpected effect. The mode incident
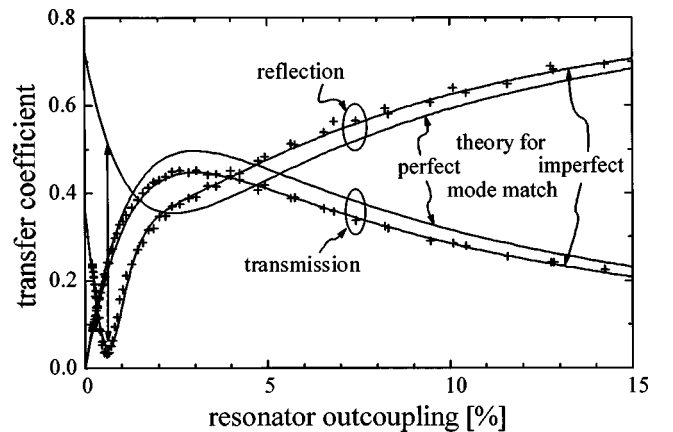
FIG. 6. Dependence of the transfer coefficients as indicated on the resonator outcoupling. Crosses: experimental data. Lines: theory. The theory that neglects imperfect mode match is wrong by an order of magnitude indicated by the vertical arrow near 0.7% of resonator outcoupling.

on the resonator may be decomposed into the part that matches the resonant mode and the orthogonal rest, which is fully reflected. This causes a very different action of the resonator on these modes. The sidebands of the resonant mode are phase shifted with respect to the carrier, those of the reflected mode are not. As the modes are orthogonal, each mode generates its own photocurrent on the detector. However, the photocurrents of the individual modes interfere. When all terms are taken into account by the generalized theory given below, quantitative agreement between experiment and theory is reached, as demonstrated in Fig. 6.

B. Generalized theory

The generalized calculation must account for several orthogonal field modes per detector. The sets D and D' denote the indices of the modes that are detected by the respective detector. According to Eq. (18), the photocurrent is then $i_D = \Sigma_{k \in D} i_k = \Sigma_{k \in D} 2A_k c_{kj} X_j$, and the generalization of $K_{kk'}(\omega, \omega)$ after Eqs. (19) and (31), is

$$K_{DD'} \equiv \langle i_D^+ i_{D'} \rangle = \sum_{k \in D, k' \in D'} A_k A_{k'} \kappa_{kk'} \delta(0)/2\pi. \quad (68)$$

Provided full linearity of the systems and decoupled quadratures, A_k is given by $A_k = c_{ki}(0)A_i$ [Eq. (17)]. Analogous to the previous arguments the expressions can be calculated for the squeezing S_D of the detected radiation, the transfer coefficient T_{Dj} from the input mode j to that detector and the correlation coefficient $C_{DD'}$ between two detected currents:

$$S_D = \sum_{k,k' \in D} A_k A_{k'} \kappa_{kk'} \Big/ \sum_{k \in D} A_k^2, \quad (69)$$

$$T_{Dj} = S_j \Big| \sum_{k \in D} A_k c_{kj} \Big|^2 \Big/ S_D \sum_{k \in D} A_k^2, \quad (70)$$

$$C_{DD'} = \frac{K_{DD'}}{\sqrt{K_{DD} K_{D'D'}}}. \quad (71)$$

If the input beams j for the system S_{kj} are uncorrelated then two expressions simplify to

$$S_D = \sum_j \Big| \sum_{k \in D} A_k c_{kj} \Big|^2 S_j \Big/ \sum_{k \in D} A_k^2 \quad \text{and} \quad (72)$$

$$C_{DD'} = \frac{\sum_j \left(\sum_{k \in D} A_k c_{kj}^* \right) \left(\sum_{k' \in D'} A_{k'} c_{k'j} \right) S_j}{\sqrt{\left(\sum_j \Big| \sum_{k \in D} A_k c_{kj} \Big|^2 S_j \right) \left(\sum_j \Big| \sum_{k' \in D'} A_{k'} c_{k'j} \Big|^2 S_j \right)}}. \quad (73)$$

Note that also these equations can be generated from the ones that neglect input squeezing by the substitution $c_{kj} \rightarrow c_{kj}\sqrt{S_j}$. Also, the carriers A_k appear as weighting factors,
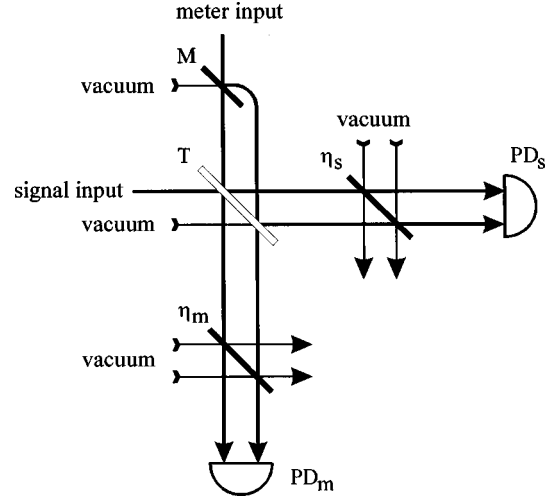

FIG. 7. Mode map for the analysis of the squeezed-light beam splitter of transmission T.

because the photocurrent generated by X_k is proportional to A_k. If there is only one bright mode ($A_k \neq 0$) per detector, these expressions reduce to those of the previous sections.

C. Application: the squeezed-light beam splitter

A seemingly simple device is the conventional beam splitter. However, complex expressions result if imperfect modematch, arbitrary squeezing and technical noise, finite beam powers, and detection losses are included. This system was investigated experimentally in detail in Ref. [15]. Here we present details of the underlying model.

We start by giving a mode map in Fig. 7 that includes all required elements and modes. This diagram represents orthogonal transverse modes by separate parallel lines. The upmost mirror is a ''Gedanken mirror'' that separates the part of the meter input that is not modematched to the signal input. Its power transmission equals the mode match of the two beams, i.e., the modulus square of the field overlap integral. The squeezings and the powers of the signal and the meter input are S_s, S_m, P_s, and P_m, respectively. Only the central mirror actually exists in the experiment, and provides a transmission T. The quantum efficiencies of the photodetectors PD_s and PD_m are simulated by mirrors of transmission η_s and η_m. Choosing a specific phase convention, e.g., the IO coefficient for the meter input to the non-mode-matched field incident on PD_s is $\sqrt{\eta_s(1-M)(1-T)}$. The experiment uses a servo loop that maximizes the output power at one detector to control the relative phase between signal and meter input. This ensures that the amplitude and phase quadratures decouple throughout the system, and provides optimum performance using an amplitude squeezed meter input. Then the quantities for the squeezing S_s^{out}, as measured at PD_s, the correlation C_{sm} between the two photocurrents and the transfer coefficient T_s from signal input to PD_s result in

$$S_s^{out} = N_s/N_s |_{S_s = S_m = 1}, \quad (74)$$

$$C_{sm}^2 = \frac{\eta_s \eta_m}{N_s N_m} [RT(M - MS_m + S_s - 1)$$

$$+ A\sqrt{MRT}(2T - 1)(S_m - S_s)$$

$$+ A^2 RT(M - MS_s + S_m - 1)]^2, \tag{75}$$

$$T_s = \eta_s T S_s (\sqrt{T} + A\sqrt{MR})^2 / N_s, \tag{76}$$

where

$$A \equiv \pm \sqrt{P_m / P_s}, \quad R \equiv 1 - T,$$

$$N_s \equiv (\sqrt{MT} + A\sqrt{R})^2 [1 + \eta_s (RS_m + TS_s - 1)]$$

$$+ (1 - M)T[1 + \eta_s (T - A^2 R)(S_s - 1)]. \tag{77}$$

N_s is the normalized noise power of the radiation incident at the detector PD_s. The expressions for S_m^{out} and the transfer coefficient T_m from the signal input to PD_m result from the substitutions $R \leftrightarrow T$, $\eta_s \leftrightarrow \eta_m$, and $A \to -A$. The sign of A reflects the choice of the relative phase between both inputs, either 0 or π.

Most notable is the special case where the beam splitter is such that $\sqrt{T} + A\sqrt{MR} = 0$. Then a complete destructive interference of the carrier of the signal beam propagating toward PD_s occurs. Its fluctuations lead to no photocurrent, and the current from the non-mode-matched part of the meter input dominates, causing T_s to vanish. In that case the squeezing at PD_s also results only from the latter beam: $S_s^{out} - 1 = (S_m - 1)(1 - M)R\eta_s$.

The dramatic degradation of the transfer coefficient in Fig. 6 is caused by a similar effect, namely, the impedance matching of the mode-matched part to the resonator that occurs at a specific resonator outcoupling. However, the situation is more complex as the non-mode-matched part also carries information from the signal beam, in contrast to the case of the squeezed-light beam splitter.

For a perfect mode match, $M = 1$, the previous results simplify to

$$S_s^{out} = 1 + \eta_s (RS_m + TS_s - 1),$$

$$S_m^{out} = 1 + \eta_m (TS_m + RS_s - 1), \tag{78}$$

$$C_{sm}^2 = \frac{\eta_s \eta_m RT(S_s - S_m)^2}{S_s^{out} S_m^{out}}, \tag{79}$$

$$T_s = \eta_s T S_s / S_s^{out}, \quad T_m = \eta_m R S_m / S_m^{out}. \tag{80}$$

Here the amplitude ratio A of both beams becomes irrelevant. Experimentally, quantitative agreement between experiment and theory is found only after taking the finite mode match into account.
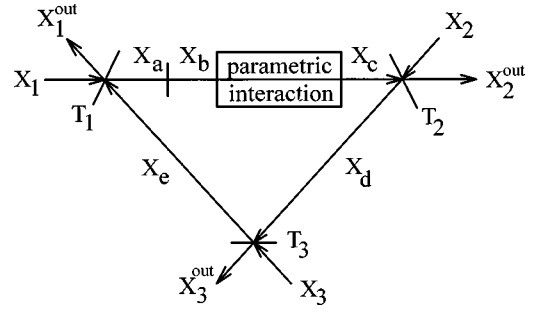

FIG. 8. Ring resonator with three coupling mirrors and parametric interaction.

XI. CALCULATION OF THE IO MATRIX FOR THE DEGENERATE OPTICAL PARAMETRIC AMPLIFIER DOPA

In this section the IO matrix for a resonant system, the degenerate OPA (DOPA) is explicitly calculated. This serves three purposes: First, it demonstrates how optical feedback that leads to resonant systems can be integrated to this formalism. Second, this approach avoids using the good cavity limit or assuming weak interactions. Third, the results are required for the specific calculations presented in Fig. 6, which compares theory to experiment and shows that finite mode match can lead to dramatic effects.

Consider the ring resonator setup of Fig. 8 with three coupling mirrors of arbitrary power reflectivites T_1, T_2, and T_3, and one parametric interaction region. If the degenerate parametric interaction is driven by a pump wave of appropriate phase, it will decouple the amplitude and phase quadratures X and Y and lead to parametric amplification factors of $e^{-p/2}$ and $e^{p/2}$, respectively. The parametric gain p depends on the pump power P_p and the nonlinearity Γ of the interaction: $p = 2\sqrt{P_p \Gamma}$. This choice of pump phase will lead to an amplitude-squeezed output state. The following calculations are sufficient for the amplitudes, the expressions for the phases are obtained by reversing the sign of p. Denoting the field operators as indicated in Fig. 8, $X_c = e^{-p/2} X_b$ results, which holds both in the time and in the frequency domain. The cavity round trip time is taken care of by $X_b(t) = X_a(t - \tau)$ which fourier transforms to $X_b(\omega) = X_a(\omega)e^{-i\omega\tau}$, where τ is the cavity round trip time and ω is the detuning from resonance. For the first mirror the quadratures are connected by $X_a = t_1 X_1 + r_1 X_e$ and $X_1^{out} = t_1 X_e - r_1 X_1$, where $r_1 \equiv \sqrt{1 - T_1}$ and $t_1 \equiv \sqrt{T_1}$ have been set. The other two mirrors work analogously, noting that the intracavity field is reflected with positive sign to ensure resonance at $\omega = 0$. This determines completely the operation of the system, and the result in the frequency domain is

$$X_a = R(X_1 t_1 + X_2 r_1 r_3 t_2 + X_3 r_1 t_3), \tag{81}$$

$$\begin{pmatrix} X_1^{out} \\ X_2^{out} \\ X_3^{out} \end{pmatrix} = \begin{pmatrix} -r_1 + RFr_2 r_3 t_1^2 & RFt_1 t_2 & RFr_2 t_1 t_3 \\ Rr_3 t_1 t_2 & -r_2 + RFr_1 r_3 t_2^2 & Rt_2 t_3 \\ Rt_1 t_3 & RFr_1 t_2 t_3 & -r_3 + RFr_1 r_2 t_3^2 \end{pmatrix} \begin{pmatrix} X_1 \\ X_2 \\ X_3 \end{pmatrix}, \tag{82}$$

where $F \equiv e^{-p/2 - i\omega\tau}$ and $R \equiv (1 - Fr_1 r_2 r_3)^{-1}$.

Note that this result does not require the assumptions of small transmissions, i.e., the good cavity limit, nor small detunings, nor small parametric gain, as long as the system is operated below threshold. Note that rate equations, which are first order approximations, are avoided. A check of the consistency relations (7) uses d as the same matrix as c except for a sign change in p. The positive outcome is not surprising since the constituents of this resonator, i.e., mirrors, time delay, and the parametric interaction pass the test individually.

The well-known equations for the good cavity limit are obtained by multiplying all transmissions ω and p with a size parameter, and taking the leading order when this parameter is small. The intuitive result for the IO relation $X_j^{\text{out}} = c_{ji} X_i$ is

$$c_{ji} = t_j R t_i - \delta_{ji}, \tag{83}$$

where the simplified resonance term is $R = 2/[L(1 + i\omega/\omega_c)]$. The total round-trip power losses are $L \equiv T_1 + T_2 + T_3 + p$, and the cavity linewidth Δf_{FWHM} (FWHM is full width at half maximum) is connected to the amplitude decay rate $\omega_c \equiv L/2\tau$ by $\Delta f_{\text{FWHM}} = \omega_c/\pi$. The OPO threshold is reached at $|p| = T_1 + T_2 + T_3$. Interestingly, relation (83) passes the consistency test (7), although the individual elements of the resonator no longer conserve the commutation relations in the good cavity limit. The reason is that the general matrix satisfies the consistency relations to any order, particularly to the leading one.

From the IO coefficients [Eq. (83)] one quickly calculates the output squeezing, the correlations, the transfer coefficients, and the conditional variance using Eqs. (33f) and (53f). These results have previously been calculated in absence of technical noise at the inputs ($S_j = 1$) by Smith et al. [22].

Note that all of these quantities including Δf_{FWHM} depend on the parametric gain p. This directly leads to a narrowing of the cavity linewidth for the antisqueezed (amplified) quadrature and to an increased bandwidth of the squeezed (deamplified) quadrature. This effect has been observed clearly in our laboratory [23].

XII. SUMMARY AND CONCLUSION

In this paper a formalism is developed that allows one to describe complex composite quantum optical systems. The approach includes technical noise by starting with time-dependent coherent input states. The input operators are then linearly propagated through a series of individual optical systems as described by their input-output relations. Finally, the output states are detected by photodetectors which generate photocurrents whose properties are analyzed in detail to obtain expressions for the squeezing [Eq. (22)], the transfer

coefficients [Eq. (24)] and the correlation coefficients [Eq. (30)]. A discussion of the connection between transfer coefficients and phase sensitivity results in a generalized criterion for phase sensitivity [Eq. (27)] for the case of two beams. An analysis of the correlation coefficient results in a necessary condition [Eq. (40)] for a system that generates entangled states. Further relations [Eq. (44)] allow one to conclude that states are entangled from experimental data even when technical noise is present.

The total correlation is introduced as a measure of the overall correlation of a set of output quadratures [Eq. (45)] and is interpreted geometrically. From this, a multidimensional uncertainty relation is derived [Eq. (50)]. Next, quantum state preparation is reviewed: The conventional approach of detection of one quadrature and modification of another is termed ''indirect'' and its optimal performance is calculated [Eq. (53)]. A different approach is to use beam splitters to superimpose quadratures and to minimize the noise on one particular quadrature. This method is termed ''direct'' QSP, and an analysis shows that the achievable minimal variance [Eq. (56)] is always smaller than the conditional variance of indirect QSP [Eq. (57)]. For the case of two beams up to 3 dB of additional noise suppression can be accomplished. Consequently it is argued that the minimal variance should be used as a criterion for QSP, rather than the conditional variance. As an application, a balanced quantum optical bus consisting of beam splitters with squeezed vacua at the usually unused ports is analyzed [Eqs. (61)–(67)].

Finite beam mode match has been shown experimentally to lead to dramatic effects (Fig. 6). To describe these, our theoretical model is further generalized to include imperfect mode match using a multimode description of a single beam. The possible interference between the photocurrents of the individual modes on a single detector results in fairly complex equations for the squeezing [Eq. (69)], the transfer coefficients [Eq. (70)] and the correlation [Eq. (71)]. Expressions for the imperfectly modematched squeezed-light beam splitter including detection losses are given [Eqs. (74)–(80)]. Finally, a direct and intuitive derivation of a general IO matrix for a degenerate optical parametric amplifier is presented [Eq. (82)].

[1] J. H. Shapiro, Opt. Lett. **5**, 351 (1980); C. M. Caves, Phys. Rev. D **23**, 1693 (1981).

[2] M. J. Collett and C. W. Gardiner, Phys. Rev. A **30**, 1386 (1984).

[3] C. M. Caves, Phys. Rev. Lett. **26**, 1817 (1982); B. Yurke, J. Opt. Soc. Am. B **5**, 732 (1985).

[4] V. B. Braginsky *et al.*, Science **209**, 547 (1980); C. M. Caves *et al.*, Rev. Mod. Phys. **52**, 341 (1980); Appl. Phys. B **64** (2) (1997), special issue on QND measurements.

[5] R. E. Slusher *et al.*, Phys. Rev. Lett. **55**, 2409 (1985); E. S. Polzik *et al.*, Appl. Phys. B: Photophys. Laser Chem. **55**, 279 (1992); G. Breitenbach *et al.*, J. Opt. Soc. Am. B **12**, 2304 (1995).

[6] M. D. Levenson *et al.*, Phys. Rev. Lett. **57**, 2473 (1986); P. Grangier *et al.*, *ibid.* **66**, 1418 (1991); S. R. Friberg *et al.*, *ibid.* **69**, 3165 (1992); J. F. Roch *et al.*, *ibid.* **78**, 634 (1997).

[7] A. Heidman *et al.*, Phys. Rev. Lett. **59**, 2555 (1987); O. Aytür and P. Kumar, *ibid.* **65**, 1551 (1990); J. G. Rarity *et al.*, Appl. Phys. B: Photophys. Laser Chem. **55**, 250 (1992).

[8] J. A. Levenson *et al.*, Phys. Rev. Lett. **70**, 267 (1993); Appl. Phys. B: Photophys. Laser Chem. **64**, 193 (1997).

[9] M. H. Holland *et al.*, Phys. Rev. A **42**, 2995 (1990); J. F. Roch *et al.*, Appl. Phys. B: Photophys. Laser Chem. **55**, 291 (1992); J.-Ph. Poizat, Ann. Phys. (Paris) **19**, 265 (1994).

[10] A. Karlsson and G. Björk, Quantum Semiclassic. Opt. **7**, 649 (1995).

[11] Z. Y. Ou *et al.*, Phys. Rev. Lett. **70**, 3239 (1993); K. Bencheikh *et al.*, *ibid.* **75**, 3422 (1995).

[12] R. Bruckmeier *et al.*, Phys. Rev. Lett. **78**, 1243 (1997); **79**, 1463 (1997).

[13] R. Bruckmeier, Ph.D. thesis, Hartung-Gorre Verlag, Konstanz, Germany, 1997 (unpublished).

[14] R. Bruckmeier *et al.*, Appl. Phys. B: Photophys. Laser Chem. **64**, 203 (1997).

[15] R. Bruckmeier *et al.*, Phys. Rev. Lett. **79**, 43 (1997).

[16] Here the term ''quantum correlation'' is used because it is caused by quantum fluctuations. We do not wish to imply that it cannot be described by classical models, such as hidden variable theories.

[17] P. Torma *et al.*, Phys. Rev. A **52**, 4812 (1995).

[18] J. Mertz *et al.*, Phys. Rev. Lett. **64**, 2897 (1990).

[19] A. S. Lane *et al.*, Phys. Rev. Lett. **60**, 1940 (1988).

[20] A. La Porta *et al.*, Phys. Rev. Lett. **62**, 28 (1989); S. F. Pereira *et al.*, *ibid.* **72**, 214 (1994).

[21] P. Torma, J. Mod. Opt. **43**, 2403 (1996).

[22] P. Smith *et al.*, Opt. Commun. **102**, 105 (1993); **106**, 288 (1994) and private communication.

[23] Klaus Schneider, diploma thesis, University of Konstanz, 1995 (unpublished).